AN EXPERIMENTAL INVESTIGATION OF BRIDGEFLOW II KERB CHANNEL UNITS

Mirali Mohammadi

Department of Civil Engineering, Urmia University
P O Box 165, Urmia 57169-33111, Iran, m.mhohammadi@mail.urmia.ac.ir

Donald W Knight

School of Civil Engineering, University of Birmingham
Edgbaston, Birmingham B15 2TT, England, d.w.knight@bham.ac.uk

David Wilson

Cast Iron Services Ltd (CIS), Woodland Road, Stanton Village, Burton-on-Tren
DE15 9TT, England, d.wilson@bham.ac.uk

(Received: March 3, 2000 – Accepted in Revised Form: July 9, 2001)

Abstract The results of an experimental investigation of kerbside bridge deck drainage units are presented. The conveyance capacity, resistance coefficients and sediment transporting efficiencies of different types of drainage unit used in shallow bridge drainage decks are examined over a range of bed gradients likely to be encountered in practice. The use of a V-shaped cross section is shown to be particularly effective in transporting sand and gravel material along the channel, and sediment threshold equations are presented. The overall hydraulic resistance of kerbside drainage units, together with the effect of joints and rib roughness on the walls of some other types of unit, is also illustrated.

Key Words Experimental Investigation, Kerbside Bridge Drainage Units, Conveyance Capacity, V-Shaped Bottom Cross-Section, Sediment Threshold, Hydraulic Resistance, Rib Roughness

چکیده در این مقاله نتایج تحقیقات آزمایشگاهی کانالهای زهکش آبهای سطحی در کنارهٔ پلها و جاده‌ها که بصورت واحدهایی بطول مشخص (نیم متر) تهیه شده‌اند، ارائه می گردد. تیپهای مختلفی از این نوع کانالها از لحاظ ظرفیت گذردهی جریان و بازده حمل رسوب در شیبهای طولی مختلف مورد آزمایش قرار گرفته‌اند. براساس این تحقیق، کانال با مقطعی شامل دیواره‌های قائم و کف V شکل برای حمل رسوبات با قطر دانه‌های مختلف مناسب می‌باشد که برای این منظور یک سری روابطی برای آستانهٔ حرکت ذرات رسوبی جهت استفاده در عمل، به دست آمده‌اند. مقاومت هیدرولیکی در مقابل جریان برای این تیپ کانالها به همراه کانالهایی با برجستگیهایی در دیواره‌های جانبی آنها مقایسه شده و تأثیر مقاومت ناشی از محل اتصال واحدهای طولی کانالها به همدیگر نیز بطور کامل تشریح و نتایج لازم ارائه شده‌اند.

1. INTRODUCTION

Stormwater may affect not only the safety of road users using bridges, but also the maintenance costs and long term integrity of the structure. A well-designed drainage channel system should intercept, collect and carry away excess water and sediment from the bridge or highway surfaces efficiently. Since most of the water in the channel system originates from surface runoff, which may last for only brief periods, the channel flow rates are typically highly variable, which may cause problems where the channels contain sediment and debris. From a hydraulics point of view, the runoff from bridges and road surfaces causes at least two major problems: (*i*) high intensity rainfall may cause high discharges of short duration which may exceed the conveyance capacity of the channel, thereby flooding the road surface; (*ii*) the surface runoff may cause sediment transport in parts of the system where there are steep channel gradients, and sediment deposition either where the channel gradients are

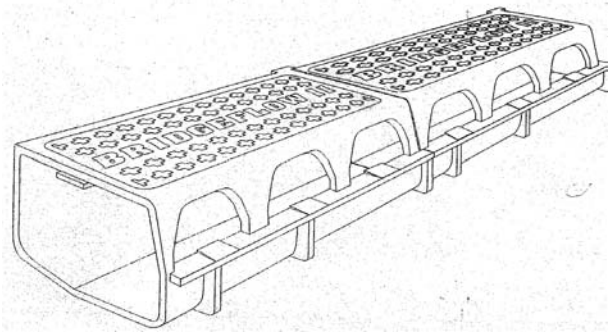

Figure 1(a). Isometric view of the CIS Bridgeflow II units.

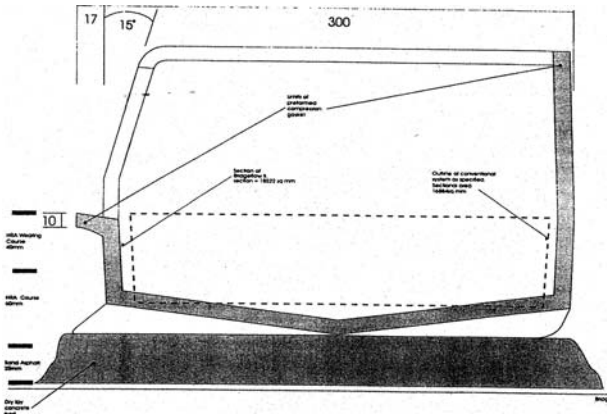

Figure 1(b). Cross section of the CIS Bridgeflow II units.

flatter or during periods of low flow. The present experimental study was concerned with both of these problems, and used two sizes of Cast Iron Services (CIS) Bridgeflow II kerb channel units as a basis for the study.

A review of the performance of 200 UK highway bridges confirmed that bridge/road surface drainage systems are often poorly designed in comparison with the structural design of the bridge [1]. Indeed, in many countries there are no procedures for the design of bridge drainage systems at all. This is surprising, given that water ingress into the bridge deck can seriously affect the long-term structural integrity of the bridge, that the skid resistance of wet surfaces is lower than that of dry surfaces, and that splashing water affects the visibility, safety and comfort of both the driver and any passengers.

Bridge drainage systems fall into two main categories, namely point and linear [2]. The following hydrologic, hydraulic and environmental factors should be considered: (*a*) design rainfall intensity; (*b*) drainage discharge capacity; (*c*) lateral inflow characteristics, (*d*) maximum permissible velocities and self-cleansing capability for sediments; (*e*) the

Figure 2 A constriction view of CIS Bridgeflow II units.

configuration of inlets, outlets, transitions and other appurtenances; (*f*) corrosion or other environmentally unacceptable conditions; and (*g*) economy of design.

This paper concerns with the hydraulic performance characteristics of two sizes of Bridge flow II kerb channel units. The experimental programme of research was conducted for CIS at the University of Birmingham, through grant GK/K56704 which formed part of the special Transport, Infrastructure and Operations (TI0) LINK programme commissioned by EPSRC in conjunction with the Department of Transport DoT in 1995. Further details are given elsewhere [3-5].

2. CIS BRIDGEFLOW II DRAINAGE UNITS

Bridgeflow II bridge drainage units are one component of a patented combined kerb/drainage system manufactured by CIS. Figure 1(a) shows an isometric view of the units and Figure 1(b) their cross sectional shape. The shape of the upper pad of the section is rectangular, and the lower pad is triangular, with the bottom vertex 20mm below the rectangular section. The units are made from ductile iron, have a maximum depth of 76mm, and manufactured sizes with nominal widths of 300 and 450mm.

Figure 2 shows a view of these units being installed on a bridge, and Figure 3 gives a view of the units after laying the bridge deck road surface. The experimental work was carried out using two sizes of unit, 300mm and 450mm, in two flumes, 9m and 15m long. Various hydraulic parameters related to conveyance capacity, resistance to flow, velocity and boundary shear stress distributions, incipient sediment motion and lateral inflow were examined. One important feature of the Bridgeflow

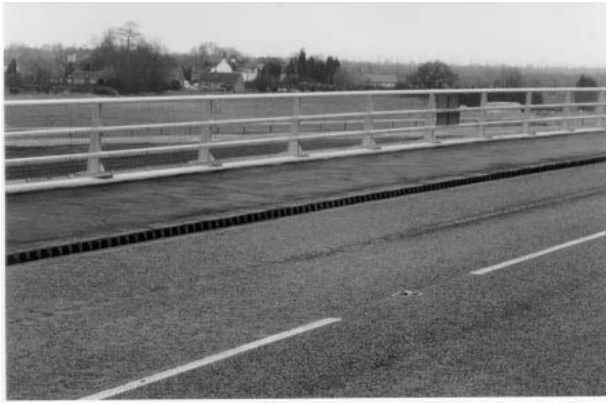

Figure 3. The finished view of the CIS Bridgeflow II drainage channel units (after road asphalting).

II channel shape is that it has a triangular lower section. This increases the channel discharge capacity at high flow depths and its sediment transportation ability at low flow depths, which are two important issues in any drainage system. Following tests with prismatic channels, under uniform flow and laterally varied flow conditions, some non-uniform flow tests were carried out, investigating flow patterns and efficiencies of different transitional sections and various bottom outlets.

The problem of leakage at joints between various types of drainage units, under different installation and temperature conditions, was examined in a large environmental chamber in parallel with the hydraulic tests. Different types of unit, and the sealing of joints between units (mastic and gaskets), were tested over a range of temperatures from -10^0C to $+50^0$C. Five Bridge flow II drainage units were placed in series to form a channel test section and exposed to a combination of the following test conditions: perfect alignment of the drainage units; misalignment of the drainage units; constant temperature; cyclic temperature variation. The CIS neoprene gaskets performed well under all these conditions, and were used in all the hydraulics tests described herein.

In addition to the hydraulic tests on two sizes of Bridgeflow II units, the opportunity was taken to perform some limited tests on some Glynwed Aquadrain units, which were of a comparable size to the 300m CIS units. These tests were of particular interest, as the Aquadrain units had a repeating pattern of circular and rectangular ribs on both sidewalls, thereby creating a rectangular cross section with heterogeneous roughness. Such sections are normally analyzed by so-called composite roughness equations [6], because the different roughness on different parts of the wetted perimeter are usually combined into a single roughness value, which will change as the depth of flow changes. Consequently, the overall resistance to flow changes with depth, as does the conveyance capacity of the channel. Data from the rectangular section, heterogeneous roughness, Aquadrain units were compared with data from the V-shaped, homogeneous roughness, CIS units. At a later stage, following the work on the CIS and Glynwed units, some further tests were undertaken on a larger specially constructed V-shaped channel, built out of PVC sheets, for more detailed studies on boundary shear stress and resistance [5].

3. EXPERIMENTAL APPARATUS AND PROCEDURES

The tests were carried out in the Hydraulics Laboratory of the School of Civil Engineering at the University of Birmingham. Tests on the 300mm CIS and Glynwed channels were undertaken in a 15m long tilting flume, and tests on the 450mm CIS channel and additional tests on the 300mm CIS channel were carried out using a specially constructed 9m tilting flume with lateral inflow, simulating runoff a roadway surface. Full details are given elsewhere by Mohammadi [5].

The experimental work was divided into four main parts, investigating the following: (1) the CIS 300mm Bridgeflow II channel units, (2) the CIS 450mm Bridgeflow II channel units, (3) the Glynwed 300mm Aquadrain channel units, and (4) a specially constructed V-shaped channel. In (3) only stage-discharge tests were carried out, and the hydraulic effects of the circular and rectangular ribs on the sidewalls of the units studied. In (4) detailed studies were made of boundary shear stress, velocity distribution and resistance, using a V-shaped channel, with a rectangular upper section, 460mm wide, and a lower triangular section with a 50m vertex, built inside the 460mm wide 15m tilting flume.

3.1 The 15m Flume The experiments were carried out under uniform flow conditions in a 15m long glass-walled rigid tilting flume having a working cross section of 460mm wide, 380mm deep with a 2.1m x 10.3m settling tank to trap sediment washed down the channel (see Figure 4).

The flume was supported by two hydraulic jacks and rotated about a hinge joint beneath the middle of the channel. The flume had a motorized slope control system, with a mechanical visual read out on a scale at the upstream end of the flume for determining the precise channel bed slope. The maximum slope obtainable was S_0=2%. Various experimental channels were built inside the flume, along the centerline, using approximately 30 individual units, each 0.5m long. Three types of channel were examined in this flume, composed of: 300mm CIS units, 300mm Glynwed Aquadrain units and a specially designed V-shaped channel, 460mm wide, made out of PVC. Figure 4 shows a channel composed of Glynwed units inside the flume.

Water was supplied to the channel through a 102mm pipeline for discharges up to 30 ls^{-1} and a 356mm pipeline for discharges higher than 30ls^{-1}. To reduce large-scale disturbances, and in order to ensure that the flow was uniformly distributed, some vertical plates and honeycombing were placed at upstream end of the flume, where the entrance tank and bell mouth shaped inlet transition section were located. However, for supercritical flow, i.e. Froude no., *Fr*>l, the honeycomb was not found to be useful and was removed. Individual trumpet shaped transition sections were built for each type of channel, and served to reduce separation and improve the development of the mean flow in the channels. Discharge measurements were made by means of a Venturi meter connected to either mercury/water or air/water manometers. An electromagnetic flow meter was also installed in the same supply line as the Venturi meter.

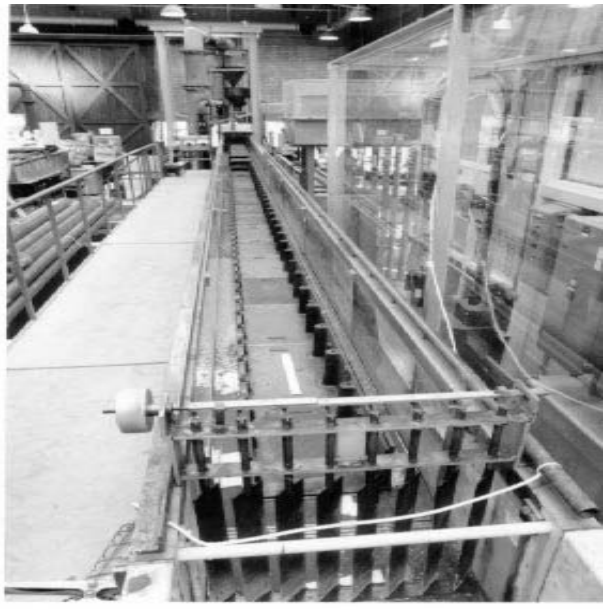

Figure 4.The 15m long experimental flume including Glynwed channel (upstream view).

Before starting any tests, levels were measured along the length of the flume, checking both the alignment of the instrument carriage rails and the various channel bed profiles. The maximum difference in the channel invert levels was found to be less than ±1.5 mm deemed to be better than the tolerance allowed when laying the drainage units in practice. A transparent, tailgate, with vertical rotating slats (see Figure 4), was installed at the downstream end of the channel in order to minimize upstream disturbance of the flow and allow a greater reach of the channel to be employed for measurement in sub critical flows. It also allowed for sediment to pass through unhindered into the settling tank beneath the flume. The test section consisted of a 12m long zone, commencing at a distance of 1.25m from the channel entrance and 1.85m from the flume entrance. However for the steepest bed slopes and largest supercritical flows, the test length was reduced to about 7m, on account of the length of the *S2* curve [7] at the inlet. An instrument trolley was mounted on rails running along the entire length of the flume. Amongst other items, this was fitted with an electrical contact depth probe, accurate to ±0.1mm, from which measurements of the water surface elevation could be made, and hence water surface slope obtained. The depth was measured at 1.0m and sometimes 0.5m intervals dong the test section. It was also possible to undertake lateral measurements using the same instrument trolley.

3.2 The 9m Flume Experiments on the larger 450mm wide CIS units were conducted in a9m long tilting flume, 1.10m wide and 0.30m deep, which was specially designed and built to undertake further hydraulic tests on all the CIS products. Figure 5 shows a view of a channel composed of 300mm CIS units, aligned on one side of the 9m long flume. The flume was designed to simulate flow in a roadway with a nominal 5% cross fall. The longitudinal slope of the flume and roadway could be varied from zero to a maximum positive gradient of 2.2%. The flume was centrally pivoted so that the slope could be set manually through two 1-tone Neeter Drive jacks, operating together.

Two pumps, with two separate delivery systems, were used to supply water to either the channel inlet, via a 150mm pipeline, or to a 9m long side weir, shown on the left hand side of Figure 5, via a 100mm pipeline. The flow over the weir and onto the road surface simulated the runoff any given rainfall intensity, thus introducing some spatially varied flow into the units, independently of any flow arisingfrom the longitudinal flow at the channel inlet. The main longitudinal flow was supplied through a 150mm pipeline using a pump with a maximum capacity of 70 ls^{-1}. Two electro-magnetic (ABB Kent-Taylor MagMaster) flow meters were installed in the separate 100mm and 150mm diameter delivery pipelines. Discharge reading accuracy in both pipelines was about 0.5%. This system thus allowed the water to be introduced not only into the channel longitudinally, but also laterally through the roadway side of the channel, thus simulating lateral runoff from a roadway surface. To avoid momentum problems and disturbances, as a result of flow exiting from the 150mm pipeline prior to entering the channel, a 1.10m × 1.25m × 0.80m inlet tank was constructed at the upstream end of the flume. In part two of the experimental programme, the experimental channel was remade using the larger 450mm CIS units instead.

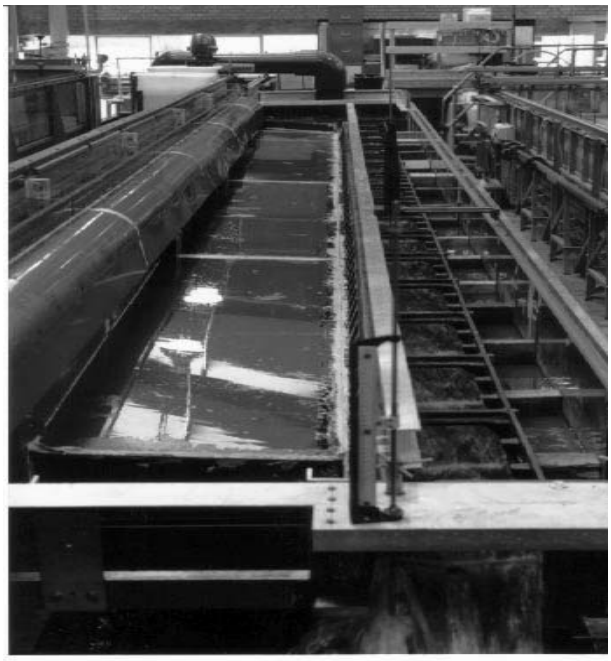

Figure 5. The 9m long tilting flume including CIS channel (upstream view).

3.3 Experimental Procedures Stage-discharge relationships for the various units were obtained for both sub critical and supercritical flows, using 5 bed slopes and approximately l0 to 20 flow depths for each slope setting. In order to obtain accurate stage-discharge and resistance relationships, it was deemed important to establish uniform flow conditions precisely. In the case of sub critical flow tests, for each slope and discharge, uniform flow was obtained by firstly undertaking a series of preliminary experiments, and plotting depth, slope and tailgate settings for several gradually varied flow M1 and M2 profiles [7]. In this way, it was then possible to estimate the tailgate setting to produce the precise normal depth for a given slope and discharge. In the case of supercritical flow tests, no downstream control was exercised through the tailgate and a free overfall condition existed. The S2 profile at the upstream end of the channel was excluded from the water surface measurements, and depth readings were only taken in that part of the channel in which uniform flow actually occurred. The same setting up procedure was followed in both the 9m and 15m flumes.

Velocity measurements were undertaken in the 300mm CIS and 460mm V-shaped channels only. A Novar 13mm diameter propeller meter (type 403, low speed) was used to measure primary velocities at pre-selected points. Isovels and lateral distributions of depth-averaged velocity were subsequently used to determine secondary flow cells, eddy viscosities and other parameters for modeling purposes. The integration of the point velocities, to give the section mean velocity, also served as an independent check on the instrumentation.

Boundary shear stress measurements were made around the wetted perimeters of the 300mm CIS units and the 460mm V-shaped channel for each of the five slopes of 0.1%, 0.2%, 0.4%, 0.9% and 1.6%. The data from the 460mm V-shaped channel are reported elsewhere 5]. The local boundary shear stress was measured using the Preston tube technique with a probe having 4.705mm outer diameter. The Preston tube was mounted on the instrument carriage and aligned vertically near the walls and normal to the bed. The tube was placed on the channel boundary at 10mm intervals on the vertical walls and every 20mm on the bed in the spanwise direction. The total pressure arising from the difference between the static and dynamic pressures was recorded by

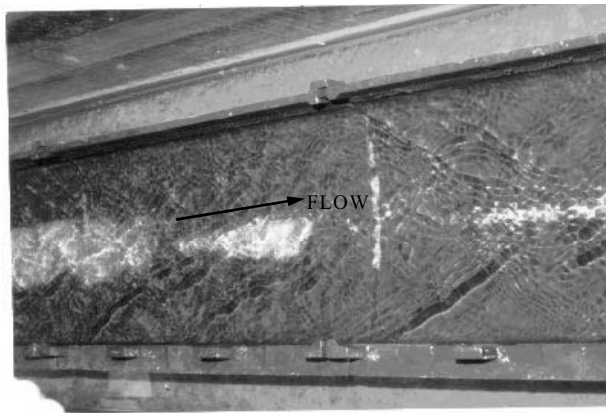

Figure 6. Sand particle movements in CIS 300mm channel.

connecting the tube to a simple manometer inclined at 12.5^0 to the horizontal line. When using the CIS units, pressure-tapping points underneath the flume could not be used because of the ductile iron channel units established on the top of the flume bed. The static pressure was therefore measured separately, using a Pitot static tube at the centerline of the measuring section, allowing at least 5minutes for it to achieve an accurate reading. However when using the 460mm V-shaped channel, two tapping holes in the bed served to give the static pressure. The differences between the total and static pressures were convened to the boundary shear stress using the Patel calibration equation [8].

In order to estimate the initiation of motion for sediment particles, tests were conducted for two sizes of material, a sand size of d_{35}=0.8mm and a road/concrete aggregate size of d_{35}=7.22mm. Sediment was placed on the bed of the channel and observations made of its mobility under flows at the same 5 slopes as used for the stage-discharge tests, plus slopes of 0.5% and 0.6%. For a given slope a discharge was set and uniform flow established. The discharge was then increased incrementally, by around 1.0 ls^{-1}, setting uniform flow each time, and the motion of the particles studied visually. When the threshold of motion occurred, the slope and discharge were recorded. Figure 6 shows an example of how sand was transported along the invert centerline in the 300mm Bridgeflow II units.

4. EXPERIMENTAL RESULTS FROM CIS 300MM BRIDGEFL0W II CHANNEL UNITS

4.1 Stage-Discharge Relationships

The stage-discharge relationships for the 300mm CIS units are shown in Figure 7 for slopes of 0.001, 0.002, 0004, 0.009 and 0.016. These slopes were adopted for these tests, so that the discharges would vary approximately in the ratio of 1, 1.414, 2, 3 and 4, on account of the square root relationship between bed slope and discharge in open channel flow. Figure 7 only shows data for flows which were contained wholly within the drainage units, i.e. H < 76mm. Additional data were obtained from similar tests in the 9m flume in which the units were allowed to overflow onto the roadway surface by the maximum permissible lateral distance of some 0.5m. This consequently extended the range of depths tested in these units from 70mm to over 100mm. The channel shape is then no longer a simple one in hydraulic terms, because of the discontinuity in hydraulic radius as the flow goes onto the roadway, and is known technically as a two-stage, or compound channel [9].

The stage discharge data was processed in a number of ways. For simple prismatic channels the relationship between depth and discharge is sometimes

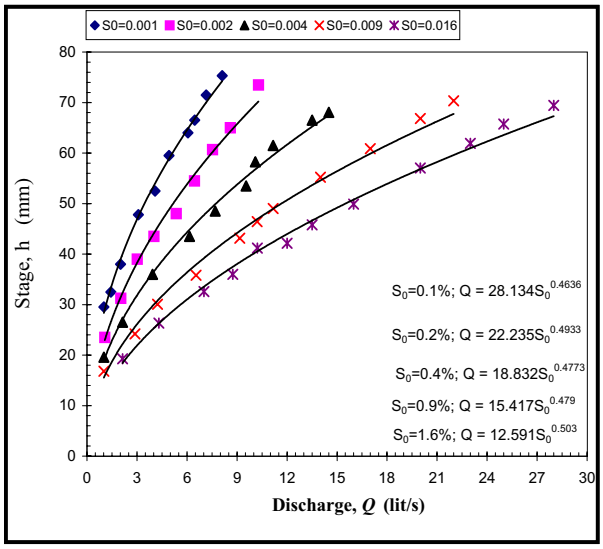

Figure 7. Stage-Discharge results together with trendlines.

TABLE 1. The Mean Values for c and n.

Slope	c	n
0.001	28.134	0.4636
0.002	22.235	0.4933
0.004	18.832	0.4773
0.009	15.417	0.4788
0.016	12.591	0.5030

written in a simple power law form as

$$H=cQ^n \quad (1)$$

where H is the stage (in mm) and Q is the discharge (in l/s and c and n are constants for a given slope setting. The mean values for c and n, based on the in-channel data alone (H<76mm) obtained from the 15m flume tests are shown in Table 1.

The data in Figure 7 show that at high stages, i.e. above 60mm and near the lip entry from the road (H=76mm), the depths are somewhat higher than those generated by the power law curve, on account of additional roughness and/or surface waves. In this region it appears that a protruding edge on the roadside of the channel interferes with the water surface, particularly when the flow is supercritical. This feature was also apparent in the stage-discharge curves for the 450mm units, undertaken later in the 9m flume.

Using all the available data for the 300mm CIS units obtained from both flumes, including that beyond the nominal, *full depth* of 76mm, and up to the maximum depth of 100mm tested with the *flooded roadway* condition, revealed that there was some interference with the flow, especially at the two lower slopes tested corresponding to sub critical flow. With the flooded roadway condition, the supporting arms at each end of a unit are of course responsible for some additional roughness, in addition to changes in channel shape. It therefore follows that more complex equations than those based on a simple power law are required for the full range of depths and flows that might be experienced in practice, ranging from in-channel flow to the flooded roadway condition. The following third order polynomials were fitted through the data and may be used in practice for the full range of depths (0<H<100mm) for these size units:

S_0=0.001 H=0.0260Q^3 -0.7959Q^2+ 11.626Q+17.899

S_0=0.002 H=0.0128 Q^3 -0.379 Q^2+ 8.0906Q+15.945

S_0=0.004 H=0.0019 Q^3 -0.1221 Q^2+ 5.0588Q+16.041

S_0=0.009 H=0.00001 Q^3 –0.0256 Q^2+ 3.2439Q+15.139

S_0=0.016 H=0.0003 Q^3 –0.0275 Q^2+ 2.6355Q+14.799 (2)

Using all the best fit curves given by Equation 2, the estimated maximum conveyance capacities of the 300mm CIS units at a depth of 76mm are as shown in Table 2, for the different slopes tested. The figures have been rounded to convenient numbers for design purposes. These values are less than those given by Equation l and the coefficients in Table 1, for the reasons stated earlier.

TABLE 2. The Estimated Conveyance Capacities at the Different Channel Slopes (CIS 300mm Units).

Slope	**Discharge** (ls^{-1}) polynomial eq. (2)	**Discharge** (ls^{-1}) power law eq. (1)
0.001	8.6	8.4
0.002	10.9	11.7
0.004	16.7	18.6
0.009	22.8	28.0
0.016	29.3	35.7

4.2 Resistance Relationships The stage discharge data were used to determine the standard resistance coefficients, Manning n or Darcy-Weisbach f equations for conveyance, given by

$$Q = AR^{2/3}S_f^{1/2} / n \quad (3)$$

$$Q = \left(\frac{8g}{f}\right)^{1/2} AR^{1/2}S_f^{1/2} \quad (4)$$

where Q=discharge, A=area, R=hydraulic radius, g=gravitational acceleration, and n and f are the section mean Manning roughness coefficient and Darcy-Weisbach friction factor, respectively. For uniform flow it has assumed that the bed slope, S_0, equals the friction slope, S_f. Figures 8 and 9 show the variation of n with Q, and f with Reynolds number, Re, for all the test data.

The average Manning n value of around 0.0095, shown in Figure 8, indicates that the CIS units are quite smooth, despite the joints. There does not appear to be a significant change in roughness with discharge or between sub critical and supercritical flow, although there is some scatter at the lowest flows tested. For design purposes a value of n=0.010 is recommended. Figure 9 show that the f values generally decrease with Reynolds number, as might be expected from the Prandtl smooth pipe law equation given by

$$1/\sqrt{f} = C_1 \log\left(\mathrm{Re}\sqrt{f}\right) - C_2 \quad (5)$$

where C_1 and C_2 are coefficients normally taken as

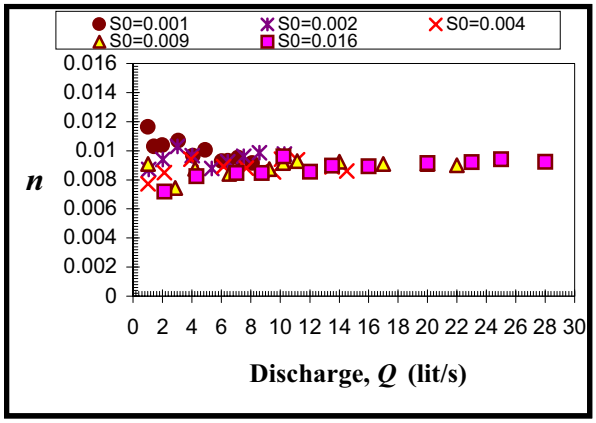

Figure 8. Manning's n v's Discharge, Q (lit/s).

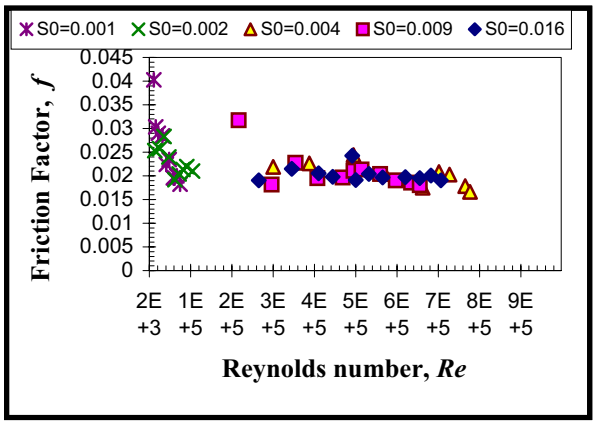

Figure 9. Friction factor, f, versus Re.

2.0 and 0.8for flow in circular pipes. This resistance coefficient is much more sensitive than the Manning coefficient, and the data again indicate the general smoothness of the CIS units. For design purposes a value of f=0.022 is recommended.

An attempt was also made to determine a resistance relationship for the CIS channel of the *standard* type given by Equation 5. Employing a linear least square regression the following equation was obtained

$$1/\sqrt{f} = 0.6326\log\left(\mathrm{Re}\sqrt{f}\right) + 4.0112 \qquad (6)$$

Comparing this equation with the Prandtl smooth pipe law indicates that both coefficients have been affected by this particular channel shape. Equation 6 was therefore modified to put it into the form of the Prandtl and Kazemipour and Apelt [10,11] equations, by fixing a value of C_1 = 2.0 or 2.12, and estimating an average value for C_2, The following equations were obtained

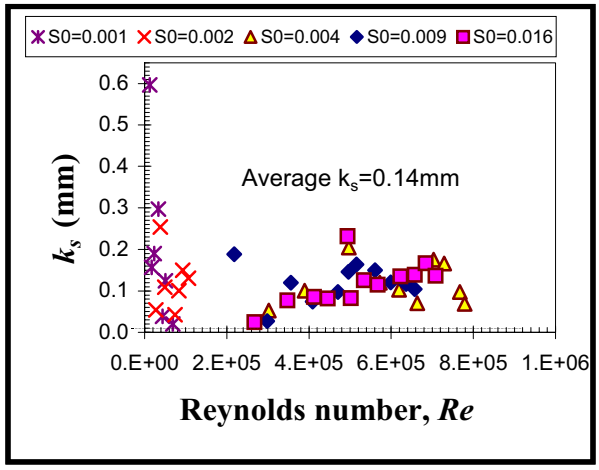

Figure 10. Values of k_s versus Reynolds number, Re.

$$1/\sqrt{f} = 2\log\left(\mathrm{Re}\sqrt{f}\right) - 2.112 \qquad (7a)$$

or

$$1/\sqrt{f} = 2.12\log\left(\mathrm{Re}\sqrt{f}\right) - 2.65 \qquad (7b)$$

The estimated value for C_2 is not radically different values from other studies in open channels.

Using the Colebrook-White pipe flow resistance equation, values of Nikurdse [3] equivalent sand roughness size, k_s, were calculated for all the tests carried out, by taking D=4R, where D=pipe diameter. The variation of k_s with Re, is shown plotted in Figure 10. As can be seen from this Figure, and comparing it with Figures 8 and 9, the k_s parameter seen to be a much more sensitive parameter than n and f. There is a large scatter among the experimental points, as is usual for such data. Consequently it is hard to estimate an average value for k_s for all the different slopes and depths tested, although k_s, like n, is meant to be a representation of the channel boundary roughness. From the experimental data, an average value of k_s=0.14mm was estimated to be appropriate for the 300mm CIS channel.

4.3 Velocity Results The point velocity measurements were integrated over the flow area to give the discharge, $Q_{int.}$, which was then compared with the discharge given by the Venturi meter, $Q_{Ven.}$. The discharge errors were expressed in a percentage form as

$$\%Q_{err.} = \frac{Q_{\mathrm{int.}} - Q_{Ven.}}{Q_{Ven.}} \times 100 \qquad (8)$$

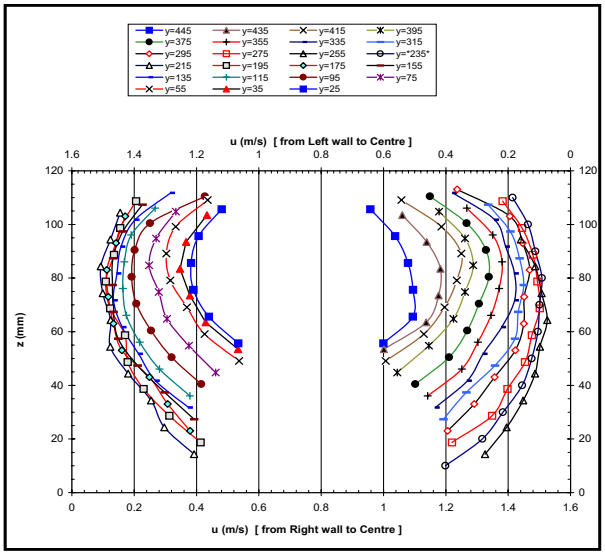

Figure 11. Velocity profiles over the depth, z, Q=51.931 l/s and S0=0.4% (V-shaped channel).

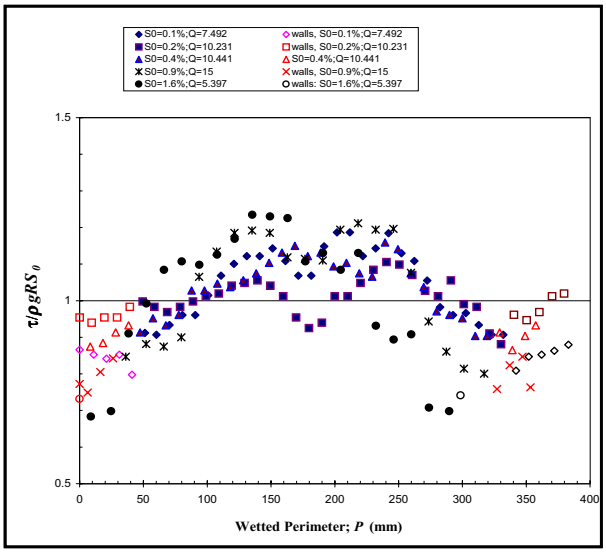

Figure 12. Dimensionless local boundary shear stress adjusted to the mean energy slope value.

Local point velocities were always adjusted to the Venturi mean values, so that when they were plotted and integrated they gave $Q_{int.}$=$Q_{Ven.}$. The discharge errors were generally very small in the case of large slopes and discharges (< 2%), but they increased for small slopes and discharges (~ 4%). The local velocities, u, measured over the flow depth, h, were also integrated to give the depth-averaged velocity, U_d. Depth-averaged velocities were then adjusted to the mean velocity and plotted against the spanwise direction, y. The local velocities were also used to construct isovel plots for selected tests.

An example of some velocity data plot is shown in Figure 11. For clarity, this velocity plot is taken from measurements in the 460mm V-shaped channel, rather than the CIS channel, as more data are available. The maximum velocity is seen to be depressed well nearby centerline as well as the free surface, an indicator of the presence of secondary flow cells [13] near the corner regions at the surface. The isovels are reasonably symmetric about the cross section centerline. Close to the boundaries, there are significant distortions due to shear and secondary flow influences [5].

4.4 Boundary Shear Stress Results Boundary shear stress measurements were made in the CIS 300mm channel for the same slopes as used for producing the stage-discharge curves. Local boundary shear stresses were integrated over the wetted perimeter, P, and the average value of boundary shear stress, $\overline{\tau}$, obtained for each test. The mean values were then compared with the energy shear stress values, $\overline{\tau_e}$, and the error in the overall shear stress calculated from

$$\%\tau_{err.} = \frac{\overline{\tau} - \overline{\tau_e}}{\overline{\tau_e}} \times 100 \qquad (9)$$

The local boundary shear stresses were also adjusted to the $\overline{\tau}$. Figure 12 shows some lateral distributions of dimensionless boundary shear stresses in the 300mm CIS units, after adjusting to the mean energy value. It can be seen from this Figure that the distributions are fairly flat along the spanwise direction for mild slope channels. However for steep channels and large discharges there are considerable perturbations in the distributions, again indicating the role of secondary flow cells [12]. More detailed analysis of boundary shear stresses in V-shaped channels is given elsewhere [5].

4.5 Incipient Sediment Motion Relationships Incipient motion of sediment particles over rigid beds is known to be different from threshold studies on beds composed of the same sediment [13]. Typical results of the CIS threshold of motion experiments, using sand and gravel, are shown in

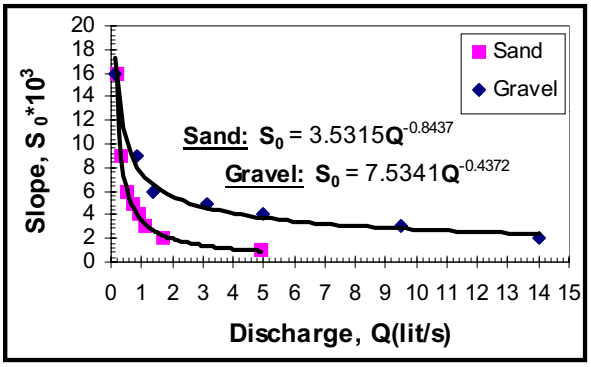

Figure 13. Threshold curves for sediment sizes d_{35} = 0.8mm and d_{35} = 7.22mm.

Figure 13. The sand and gravel appear to behave in a similar way on rigid beds, with larger values of bed slope required at small discharges to ensure movement or no deposition. From the data the following equation was obtained for incipient motion for the sand size having d_{35}=0.80mm

$$S_0 = 0.0035315\ Q^{-0.8437} \quad (10)$$

For the aggregate material size having d_{35}=7.22mm, the corresponding equation was

$$S_0 = 0.0075341\ Q^{-0.4372} \quad (11)$$

where S_0 is the channel bed slope and Q is discharge in ls^{-1}. For a given discharge, if the bed slope is less than that given by the appropriate equation then there is no motion. Alternatively for a given slope the minimum discharge (or velocity) that induces sediment motion can be calculated from the same equation.

An attempt was made to compare the experimental data with the Shields [14] criterion for threshold and the Ackers and White [15] bedload transport formula with the imposed condition of $A=Fgr$, where A=function depending on dimensionless grain size, and Fgr = sediment mobility number. The results are shown in Figures 14 and 15 for sand and gravel respectively.

As can be seen from these two Figures, both materials show close agreement with the Ackers and White equation. The Shields approach is good for sand size particles but not so for large aggregate particles. Having shown that the Ackers and White equation predicts the threshold quite well for sand and gravel over a range of depths, slopes and discharges, it is suggested that this formula can be used for other sediment sizes and slopes with a certain degree of confidence.

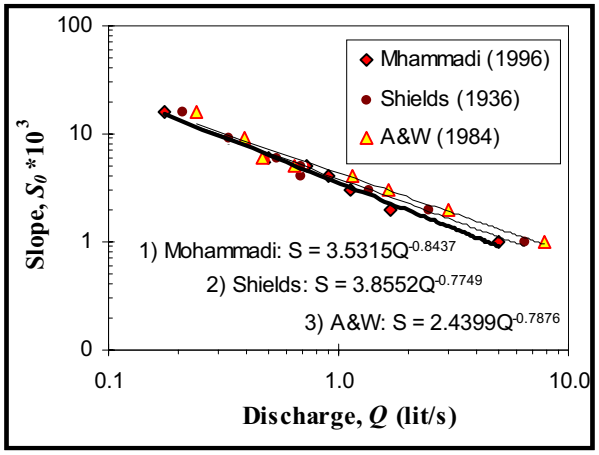

Figure 14. Comparison of the threshold condition d_{35} = 0.8mm with Ackers and White and Shields.

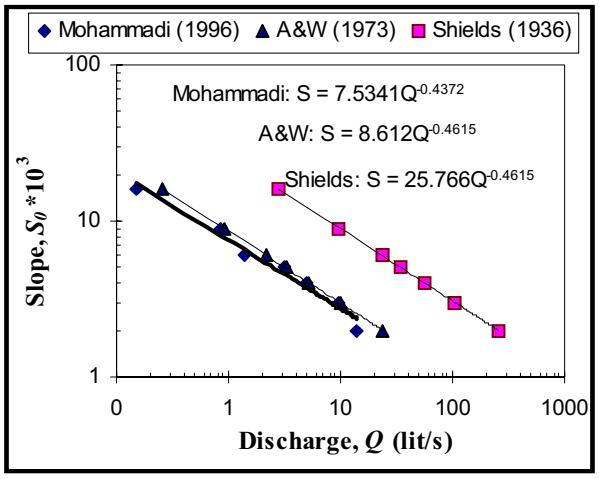

Figure 15. Comparison of the threshold condition d_{35}=7.22mm with Ackers and White and Shields.

5. EXPERIMENTAL RESULTS FROM CIS450MM BRIDGEFL0W II CHANNEL UNITS

5.1 Stage-Discharge Relationships A series of tests was undertaken in the 9m flume using 450mm CIS units in order to compare their performance with the 300mm CIS units. The cross section of the larger units was similar to the 300mm units shown in Figure 1(b), with the exception that the internal width was 415mm.The change in invert height was the same at 20mm,as

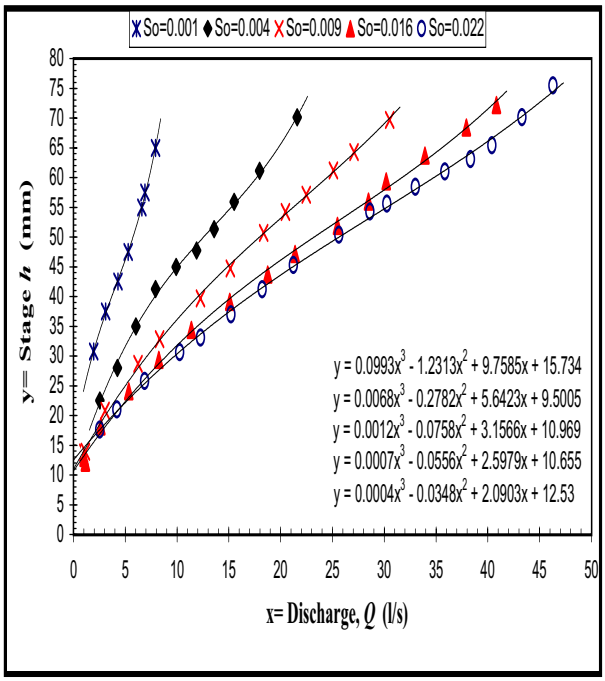

Figure 16. Stage-Discharge results (CIS 450mm channel).

TABLE 3. The Estimated Power Law Equation Coefficient at the Different Channel Slopes (CIS 450mm Units).

Slope	*c*	*n*
0.001	20.929	0.5182
0.002	13.979	0.5201
0.004	12.693	0.4782
0.009	11.454	0.4738
0.016	9.9509	0.5050

TABLE 4. The Estimated Conveyance Capacities at the Different Channel Slopes (CIS 450mm Units).

Slope	**Discharge** (ls^{-1}) polynomial eq. (2)	**Discharge** (ls^{-1}) power law eq. (1)
0.001	9.0	12.0
0.002	23.3	25.9
0.004	33.1	42.2
0.009	43.5	54.3
0.016	47.4	56.0

was the maximum depth of 76mm, measured from the lowest point on the invert to the lip. Because of the increased width, the invert crossfall slope for the 450mm units was smaller than the 300mm units.

The stage-discharge relationships are shown in Figure 16 for slopes of 0.001, 0.004, 0.009, 0.016 and 0.022. Some of these slopes are identical to those used in earlier tests, but because the 9m flume was capable of being set at a steeper gradient an extra slope of 0.022 was tested. Because the 9m flume was considerably shorter than the 15m flume the length available for uniform flow to become fully established was much reduced, particularly for supercritical flow.

As shown by Figure 16 and noted previously, a simple power law would not fit the data well at high depths on account of the small internal ribs near the lip. In order to illustrate this, best-fit power law equations, based on Equation 1, were fitted to the data and gave the coefficients shown in Table 3.

The best-fit polynomial functions, shown in Figure 16, are given by:

$$\begin{aligned} S_0{=}0.001 \quad & h{=}0.0993Q^3 - 1.2313\,Q^2 + 9.7585\,Q + 15.734 \\ S_0{=}0.004 \quad & h{=}0.0068\,Q^3 - 0.2782\,Q^2 + 5.6423\,Q + 9.5005 \\ S_0{=}0.009 \quad & h{=}0.001\,Q^3 - 0.0758\,Q^2 + 3.1566\,Q + 10.969 \\ S_0{=}0.016 \quad & h{=}0.0007\,Q^3 - 0.0556\,Q^2 + 2.5979\,Q + 10.655 \\ S_0{=}0.022 \quad & h{=}0.0004\,Q^3 - 0.0348\,Q^2 + 2.0903\,Q + 12.530 \end{aligned} \tag{12}$$

Using all the best-fit curves given by Equation 12, the estimated maximum conveyance capacities of the 450mm CIS units at a depth of 76mm are as shown in Table 4, for the different slopes tested. The figures have been rounded to convenient numbers for design purposes.

These values are less than those given by Equation 1, based on a simple power law, and the coefficients in Table 3 for the reasons stated earlier. Since the actual widths of the 300mm and 450mm units were 278mm and 415mm respectively, the results should scale by the factor 415/278(=1.4928), which is seen by comparing Tables 2 and 4 to be approximately true. Based on the power law functions, the results actually scale by a actor of 1.454. The reasons why they might not be quite in proportion are because of the different invert crossfall slopes and surface finishes, giving slightly different roughness values.

5.2 Resistance Rrelationships The stage discharge data were again used to determine the resistance coefficients, f and n. The Manning n data for discharges up to 50 l/s are shown in Figure 17. A comparison of Figures 8 and 17 shows that the 450mm units were slightly rougher than the 300mm units. It is thought that this was due to the different quality of the joints between individual

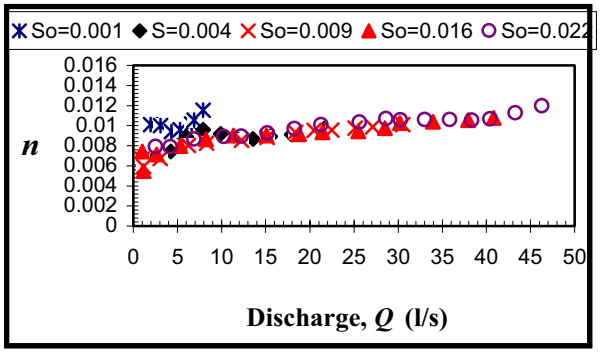

Figure 17. The Manning n versus Q (CIS 450mm channel).

units. There is also a slight difference in the variation of Manning n with discharge for the two sizes of units. Figure 8 shows a very slight decrease in n with Q whereas the opposite is true for the larger size units. For design purposes, these variations are very slight. In terms of the more sensitive Darcy-Weisbach coefficient, a f value of 0.025 is recommended for the 450mm units, which is around 12% higher than the value of 0.022 for the 300mm units. Such differences are immaterial in practice, as sediment and debris would make much larger roughness changes.

6. EXPERIMENTAL RESULTS FROM 300MM GLYNWED AQUADRAIN CHANNEL UNITS

In order to investigate the discharge capacity and resistance of a channel made of units of a comparable size as the CIS units but with different roughness characteristics, a similar series of tests was undertaken in the 15m long tilting flume using 300mm Glynwed Aquadrain units.

6.1 Stage-Discharge Relationships Uniform flow was established for the various discharges and slopes, and the normal depths obtained in the manner indicated previously. To ensure comparability with the 300mm CIS channel data, the same five bed slopes of 0.1%, 0.2%, 0.4%, 0.9% and 1.6% were used. The results are shown in Figure 18.

Experimental discharges were pre-selected at certain depths in order to give a comprehensive h versus Q curve. In the time available, and given the small size of the channel, together with the ribs on the wall surfaces, meant that only four discharges could be tested for the case of mild slopes (S_0=0.1%), and up to eight discharges for the steeper slopes. A

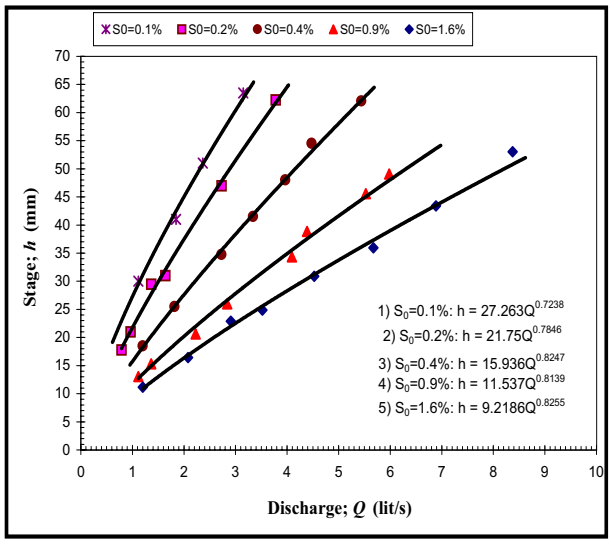

Figure 18. Stage-discharge results (Glynwed channel).

comparison of the stage-discharge results for the Glynwed and CIS channels is shown in Figure 19. This Figure shows that the discharge capacity of the CIS 300mm channel is much higher than that of the Glynwed one, especially as the depth and slope increase.

6.2 Roughness Analysis The roughness of the channel made up of Glynwed Aquadrain units was analyzed in more detail than the ones made up of CIS units, on account of its composite nature. The variation of Manning n with discharge and depth are shown in Figures 20 and 21, respectively. Figure 20 shows that the n increases slightly with Q, and Figure 21 shows that n increases significantly with h, arising from the increasing influence of the rib bed walls. Some analysis of these overall resistance coefficients was therefore attempted using three different approaches.

The first approach was based on calculating the form-drag of the individual rib elements on each sidewall, using the equations and Figures given by ESDU 16]. Values of the Manning roughness, n_l=0.40 and n_r=0.020, were determined for the left and right walls (circular and rectangular rib elements) respectively [4,5]. Since the channel units were made of cast iron, the Manning n for the bed was taken as 0.010, estimated as a mean value from the CIS channel data. Using these values, and applying the Pavlovskii composite roughness equation [6], the calculated overall values of n = 0.020 and f=0.092 were obtained at about full depth i.e.

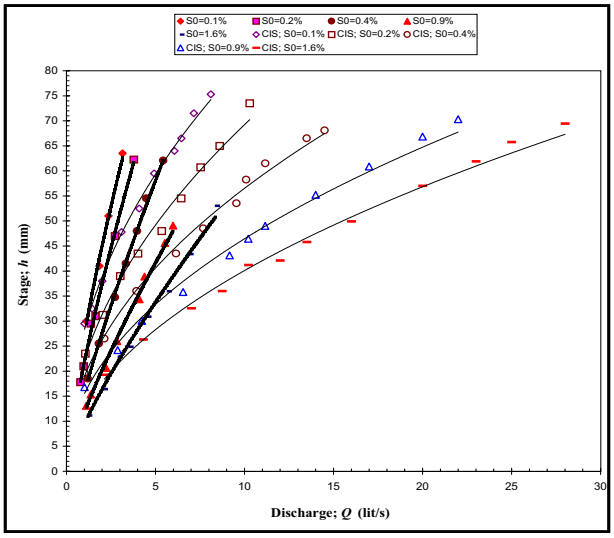

Figure 19. A comparison: stage-discharge curves for CIS 300mm and Glynwed channels.

h=65mm. Different composite roughness values apply at other depths, and could be calculated in order to predict the stage-discharge relationships.

The second approach was based on using a number of alternative composite roughness equations, other than the Pavlovskii one. In all, ten equations were examined [5], mostly based on shear force [l7] or resistance analysis [18,19]. In almost all methods, slope, velocity and hydraulic radius of the sub areas are assumed to be equal to the overall mean values i.e. U_i=U, S_{0i}=S_0 and R_i=R. According to the previous section, the values of the Manning roughness coefficients, n_l=0.040, n_r=0.020, and n_b=0.010 for the channel left wall, right wall and bed respectively, were adopted. Inserting these values into the composite roughness equations, values of composite roughness coefficient, n_c, for the Glynwed channel were calculated for the same flow depths and slopes as the experimental data and the flow discharges computed.

The mean error and standard deviations indicated that the Pavlovskii method was the most suitable for the Aquadrain units, probably on account of their simple geometry and well defined roughness on each sidewall. Although the Pavlovskii equation gave good results for mild slopes i.e. 0.1% and for shallow depths for every slope, for larger depths and slopes the agreement was not so good. This is thought to be due to *choking* phenomenon [7] in supercritical flow at the highest slope. When the flow *chokes* between roughness elements, a series of hydraulic jumps form along the channel in a repeatable manner.

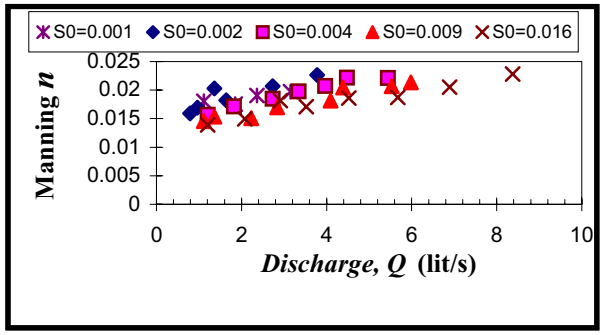

Figure 20. Manning n versus Q for the Glynwed channel.

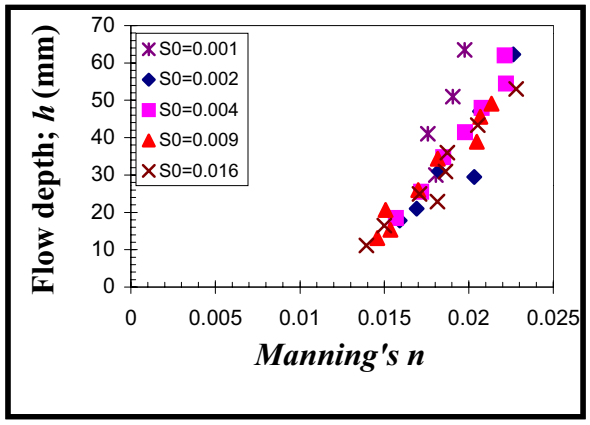

Figure 21. Manning n versus h for the Glynwed channel.

The third approach was to use a discharge adjustment function (*DAF*). The variation of the Manning n with stage, h, for all the different slopes considered showed that the value of n increases with increasing flow depth. Accordingly, the discharge adjustment function (*DAF*) was defined as a function of flow depth, h, by plotting ζ=Q/Q_{pred} versus h, as shown in Figure 22, and this resulted in the following equation

$$\zeta = 2.719h^{-0.2651} \qquad (13)$$

where Q is the dischargefrom the experimental results, and Q_{pred} is the calculated value based on using a constant value of n=0.020 or f=0.092. Discharges calculated by using *DAF* are compared with the observed discharges in Figure 23. As can be seen, there is only a small amount of scatter. It appears therefore that this function gives an improvement in use of the simple lD Manning equation and results in a better design for simple and compositely roughened channels. It seems that

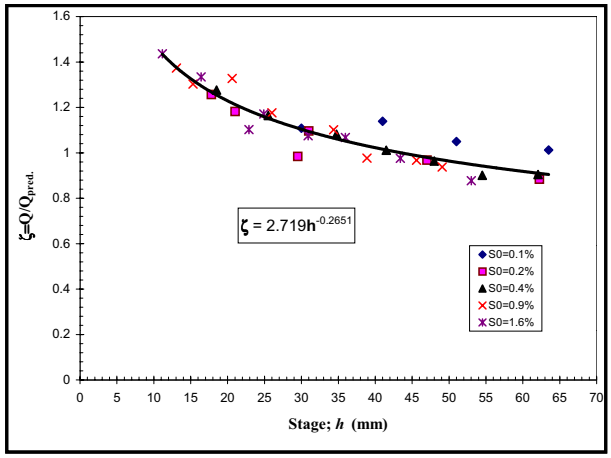

Figure 22. Definition of *DAF* as a function of stage, *h*.

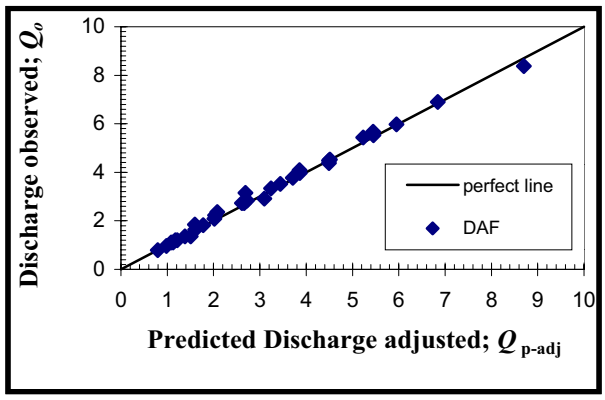

Figure 23. A comparison between discharges (observed and adjusted by *DAF* for the Glynwed channel).

in principle a *DAF* could be determined for any channel shape, including different roughness sizes based on the Manning equation, and used to calculate conveyance capacities at any flow depth.

7. DISCUSSION OF THE RESULTS

The experimental facilities have proved to be effective in obtaining conveyance capacity, resistance, and sediment threshold results for both sub critical and supercritical flows in various bridge deck drainage units. The cross sectional shape of the Bridgeflow II kerb units has been shown to have some good design features in relation to high flows, low flows, spatially varied flows and self-cleansing capabilities. Units with deliberate installation defects had only minor effects on the overall efficiency of the system. The CIS system is shown to be hydraulically efficient compared with other contemporary designs.

The resistance values of the CIS units shown in Figures 8 and 9 indicate that the units are surprisingly smooth, and that very little further advantage would be gained by additional processing of the surface finish. In one series of tests the joints between the 450mm CIS units were laid less precisely than those between the 300mm CIS units, in order to replicate poor site laying conditions, and gave only an average 5% increase in roughness.

The resistance values for the Glynwed Aquadrain units shown in Figures 20 and 21 indicate that the units are considerably rougher than the CIS units. A composite roughness value has to be calculated for each depth of flow prior to using it in a discharge equation, as the bed and walls of the units have different roughness values, arising from the rib elements. The Pavlovskii composite roughness equation appears to give reasonable results when predicting the stage-discharge relationships for such units. Alternatively, a discharge adjustment function (*DAF*) based on the depth variation of resistance, may be used.

Figure 19 shows that the conveyance capacity of the Glynwed units is significantly less than the CIS units, despite having a flat bed and a greater theoretical flow area at low depths. This is mainly due to the relatively large rib roughness elements on both sidewalls of the Glynwed units, rather than differences in width (255mm compared to 278mm). A direct comparison of either the stage-discharge curves (see Figures 7 and 18) or the resistance values (Figures 8 and 20) serves to show these differences. Using a target depth of 50mm. Table 5 shows a direct comparison of the conveyance capacities for the two types of unit.

Table 5 shows a loss of capacity of around 43%, averaged for all slopes, in comparison with the CIS units. It should be noted that if a higher depth had been chosen as the reference value, then the differences would have been larger, since more of the wetted perimeter would have been affected by the rib roughness. This highlights the act that two similar sized units can have very different flow capacities, a feature often ignored by practitioners.

The incipient sediment transport tests, using sand and gravel, showed the high efficiency of the V-shape channel in aiding the removal of sediment under various flow conditions. Further tests using cohesive sediments would be desirable, in order to

TABLE 5. A Comparison of Discharges for the CIS and Glynwed Channels

Slope	CIS (l/s)	Glynwed (l/s)	Differences (%)
0.001	3.480	2.312	-33.6
0.002	5.089	2.889	-43.2
0.004	7.735	4.158	-46.2
0.009	11.678	6.306	-46.0
0.016	15.512	8.214	-47.0

simulate all possible conditions found in practice. The presence of ribs on sidewalk was found to create some faster flow at the channel centerline, but zones of re-circulating flow near the walls where sediments could deposit.

Extensive testing of various sealing systems between units showed that the widely used mastic sealant was ineffectual with regard to leakage. The most efficient sealant type and size, and the one preferred by CIS, was a 9mm square neoprene gasket. This gasket would typically be fitted in the factory, giving additional assurance of the efficacy of the sealant application. The points raised previously highlight the need to upgrade the specification for bridge drainage systems. In view of the variation in results produced by different systems, it is suggested that the following should be incorporated into a specification in order to provide a performance *benchmark* against which the systems can, with supporting evidence, be measured.

Structural load performance - All units including expansion units to be made of ductile iron units to conform to the loading requirements of BS EN124D400. The approved system should have a known reputable third party accreditation, such as BSI Kitemark.

Conveyance capacity - For design of the flow characteristics of any proposed system, suppliers must state the Manning roughness of their units. Assumed values are not considered acceptable. The following parameters should be derived from laboratory flume tests:
- a composite Manning roughness for each type of unit;
- the variation of n with discharge, depth, Reynolds number and Froude number;
- longitudinal depth profiles using spatially varied flow tests.

Leakage - Any proposed sealing system shall only be acceptable if laboratory tests have demonstrated their efficiency under cyclic temperature testing for the intended application. Factory fitted gaskets are to be preferred.

Sediment built up – Any proposed system shall demonstrate that it is efficient in removing sediment and in avoiding deposition.

Outfall and diversions - The efficiency of any proposed outfall system shall be demonstrated from laboratory tests.

Supporting evidence, ideally third party, should be available to support these claims. Each of the above are proving obstacles to getting properly designed drainage systems on our bridges. In addition, the move to DBF0 (design, build, finance and operate) means that single point inlets to carrier pipes are being used, without accurate review of their efficiency.

The overall strategy of removing water from a bridge deck needs thinking out afresh. In particular the passage of water of the roadway surface, into the kerbside unit, down a diversion structure, along some drainage pipe and onto the outlet needs modeling in its entirety rather than treating each component in isolation. As shown by the diversion tests, not reported herein, there may be a critical point in the overall system that may significantly affect the whole performance.

8. CONCLUSIONS

From these tests the following conclusions are drawn:

1. Mean stage discharge relationships, based on a simple power law, have been determined for three types of kerbside drainage units, namely 300mm and 450mm CIS units and a 300mm Glynwed unit.

2. The simple power law relationship, based on Equation 1, generally fits the Glynwed data well, but only fits the CIS data up to depths of 60mm. For depths in excess of 60mm, third order polynomial relationships, based on Equations 2 and 12 were found to be necessary to describe the

complete stage-discharge relationship for both sizes of CIS unit, including that part for the flooded roadway condition.

3. The maximum conveyance capacities of the CIS units are given in Tables 2 and 4 for different bed slopes ranging from 0.001 to 0.022. Both sub critical and supercritical flow conditions have been tested, covering Froude numbers from 0.5 to around 2.3.

4. The results suggest that for design purposes the drainage capacity of the 300mm CIS units may be increased by at least 50%, if the 0.5m flooded roadway condition is permitted. It is likely that a similar increase will apply also to the 450mm CIS units.

5. The resistance values for the 300mm CIS units are surprisingly smooth in their ductile iron form, including joints. It therefore follows that no further advantage would be gained by further additional processing of the surface finish of the units and joints. For design purposes a Manning n value of 0.010 or a Darcy-Weisbach f value of 0.022 may be safely assumed. Slight imperfections in invert alignment of adjacent units which may occur in the laying process have been found to have little effect on the hydraulic performance of the channels, increasing the roughness by only some 5%.

6. The resistance values of the CIS units do not appear to vary markedly with depth, unlike the Giynwed units which show a strong depth dependence (see Figure 21). The two rib elements on the walls of the Glynwed units are clearly responsible for this effect. The composite Manning n value, and its variation with depth, may be determined by the Pavlovskii formula. Alternatively, a discharge adjustment function (DAF), based on the depth variation of resistance, may be used.

7. The results show that units manufactured from similar materials and with comparable dimensions will not have the same conveyance capacity. The configuration and roughness of any internal channel faces are also clearly very important. It therefore follows that when a channel is no longer a *simple* one in hydraulic terms, i.e. it is either a *compound* channel (as in the flooded roadway case) or a *composite* one (as when the flow area is divided by internal walls), the expected flow rates will be significantly lower than those expected from calculations based on the total flow area and roughness. Care should therefore be exercised with some new Bridge drainage systems which have such channels. Their capacity can only be fully assessed by laboratory flume tests.

8. A direct comparison of either the stage-discharge curves (see Figure 19) or the resistance values serve to show the differences in the conveyance capacities of the two types of unit tested herein. Table 5 shows that the 300mm Glynwed units are around 43% less efficient in discharging water at a depth of 50mm in comparison with the 300mm CIS units. The rib roughness is clearly the main contributory factor to this loss of conveyance capacity.

9. The velocity profile data and isovles indicate that the maximum velocity does not necessarily occur at the free surface. This is evidence of the presence of secondary currents, caused by the shape of the cross section.

10. Plots of local boundary shear stress against wetted perimeter show that the distributions are fairly uniform for the case of mild slopes. For steep channel slopes, especially for large discharges, the maximum boundary shear stress does not necessarily occur at the section centerline. Some significant perturbations were observed also to occur, again indicating the influence of cross sectional shape and secondary currents.

11. The results of the threshold of motion experiments indicate that a relationship of the form given by a power law between S_0 and Q, is suitable for defining the incipient motion of both sand and gravel particles (see Equations 10 and 11 and Figure 13).

12. An attempt was also made to use the Shields (1936) threshold criterion and the Ackers and White (1973) sediment transport equation with the imposed condition of $A=F_{gr}$. The results show that the Ackers andWhite equation is more suitable than the Shields one. It is therefore suggested that the Ackers andWhite formula may be used for

other sediment sizes and channel bed slopes with a certain degree of confidence (see Figures 14 and 15).

9. ACKNOWLEDGEMENTS

The experimental program of research work was conducted for CIS at the University of Birmingham, through grant GK/K56704 which formed part of the special Transport, Infrastructure and Operations (TI0) LINK program commissioned by EPSRC in conjunction with the Department of Transport (DoT) in 1995. The authors gratefully acknowledge their financial support. Cast Iron Services (CIS Ltd) funded the combined kerb/drainage project, and their collaboration is greatly appreciated by the two first authors. The first author also greatly acknowledges his sponsors: the Ministry of Science, Research and Technology of Iran and the University of Urmia.

10. NOTATION

A	area; constant in Ackers and White equation
c	coefficient
C	coefficient
d	sediment size
DAF	discharge adjustment function
F	Darcy-Weisbach friction factor
Fgr	sediment mobility no. in Ackers and White equation
Fr	Froud number
g	acceleration due to the gravity
H	local water depth of channel
h	water depth of the triangular bottom section
k_s	Nikuradse sand equivalent roughness size
n	Manning roughness coefficient, a coefficient
P	wetted perimeter
Q	flow discharge
R	hydraulic radius or conveyance depth
Re	Reynolds number ($=4UR/\upsilon$)
S_0	longitudinal bed slope
S_f	friction slope
u	local velocity
U	mean section velocity
U_d	depth-averaged velocity
x	streamwise direction
y	spanwise direction
z	direction normal to the xy plane;
ρ	water density;
ζ	discharge adjustment function (DAF), (Q/Q_{pred})
τ_b	boundary shear stress;
τ_e	boundary shear stress of mean energy slope
τ	average boundary shear stress.

11. REFERENCES

1. Wallbank, E. J., "The Performance of Concrete Bridges: a Survey of 200 Highway Bridges", ***A Report for the Dept. of Transport***, G Maunsell andPartners, (1989), 1-89.
2. Mohammadi, M., "An Introduction to Bridge Drainage Hydraulics", ***Proc. 2nd International Conference on Bridges,*** Amir Kabir University of Technology, Tehran, Iran, (September, 1996). 10-12
3. Knight, D. W. and Freer-Hewish, R. J., "Performance Characteristics of Bridgege Flow Kerb Channel Units for the Drainage of Bridge Pavement Surfaces", ***Final Report for EPSRC on Grant GR/K56704***, The University of Birmingham, (June, 1997), 1-20.
4. Knight, D. W., "Performance Characteristics of Bridge Flow Kerb Channel Units for Drainage of Bridge Pavement Surface", ***Final Report on Hydraulics Performance Tests for CIS***, The University of Birmingham, (March 1997), 1-160.
5. Mohammadi, M., "Resistance to Flow and the Influence of Boundary Shear Stress on Sediment Transport in Smooth Rigid Boundary Channels", PhD Thesis, School of Civil Engineering, The University of Birmingham, England, (1998).
6. Yen, B. C., "Hydraulic Resistance in Open Channels", in Channel Flow Resistance: Centennial of Manning formula, (Ed. Yen B.C.), Water Resources Publication, Colorado, USA, (1992), 1-136.
7. Henderson, F. M., "Open Channel Flow", Macmillan, New York, (1966).
8. Patel, V. C., "Calibration of the Preston Tube and Limitations on its Use in Pressure Gradients", ***Journal of Fluid Mechanics***, Vol.23, Part 1, (1965), 185-208.
9. Knight, D. W. and Shiono, K., "River Channel and Floodplain Hydraulics", Chapter 5, Floodplain Processes, Eds.: Anderson, Walling and Bates, J Wiley, Chichester, (1996), 139-181.
10. Kazemipour, A. K. and Apelt, C. J., "Shape Effects on Resistance to Flow in Smooth Rectangular Channels", Dept. of Civil Eng., University of Queensland, Australia, Research Report Series No.CE9, (April 1980).
11. Kazemipour, A. K. and Apelt, C. J., "New Data on Shape Effects in Smooth Rectangular Channels", ***Journal of Hydraulic Research***, Vol. 20, No.3, (March 1982), 225-233.
12. Knight, D. W., Yuen, K. W. H. and Alhamid, A. A. I**.,** "Boundary Shear Stress Distributions in Open Channel Flow", *in* ***Physical Mechanisms of Mixing and Transport in the Environment***, Eds.: K. Beven, P. Chatwin and J. Millbank, J. Wiley, Chidester, Chapter 4,

(1994), 51-87.
13. Novak, P. and Nalluri, C., "Incipient Motion of Sediment Particles over Rigid Beds", ***J. of Hydraulic Research***, IAHR, Vol. 22, No.3, (1984), 181-197.
14. Shields, A., "Anwendung der Anelichkeismechanik und der Turbulenze forschung auf die Geschiebebewegung (Application of Similarity Principles and Turbulence Research to Bed Load Movement)", Mitteilungen 26, Preussischen Versuchsanstalt fur Wasserbau and Schiffbau, Berlin, (Translated to English by W.P. Ott and van Uchelen, California, Institution of Technology, Pasadena, CA., (1936).
15. Ackers, P. and White W. R., "Sediment Transport: New Approach and Analysis", ***J. Hydraulics Div.***, ASCE, Vol. 99, HY11, (November 1973), 2041-2061.
16. Engineering Science Data Unit (ESDU), "Losses Caused by Friction in Straight Pipes with Systematic Roughness Elements", Item No. 79014, (1979), London.
17. Rhodes, D. G., and Knight, D. W., "Distribution of Shear Force on Boundary of Smooth Rectangular Duct", ***J. Hydraulic Engineering***, ASCE, Vol. 120, No. 7, paper No. 6195, (July 1994), 787-806.
18. Alhamid, A. A. I., **"**Boundary Shear Stress and Velocity Distributions in Differentially Roughened Trapezoidal Open Channels"**,** PhD Thesis, University of Birmingham, Birmingham, England, (1991).
19. Knight, D. W., Alhamid, A. A. I; and Yuen, K. W. H., "Boundary Shear in Differentially Roughened Trapezoidal Channels", in Hydraulic and Environmental Modeling: Estuarine and River Waters, Ch. 1, Eds.: R. A. Falconer, K. Shiono, and R. G. S. Mathew, Ashgate,, (1992), 3-14.